

# Supramolecular Assemblies of Trinuclear Copper(II)-Pyrazolato Units; A Structural, Magnetic and EPR Study

Kaige Shi, Logesh Mathivathanan, Radovan Herchel, Athanassios K. Boudalis, and Raphael G. Raptis

**Table S1.** Crystallographic and refinement data for [1] and [2].

	[1], CCDC2005300	[2], CCDC2005301
Empirical formula	C <sub>170</sub> H <sub>148</sub> Cl <sub>8</sub> Cu <sub>7</sub> N <sub>26</sub> O <sub>2</sub> P <sub>4</sub>	C <sub>45</sub> H <sub>40</sub> Cu <sub>3</sub> N <sub>16</sub> OP <sub>2</sub>
Formula weight	3439.40	1073.49
Temperature/K	293(2)	200(2)
Crystal system	triclinic	monoclinic
Space group	<i>P</i> $\bar{1}$	<i>P</i> 2 <sub>1</sub> / <i>c</i>
<i>a</i> /Å	14.161(7)	8.6121(9)
<i>b</i> /Å	17.814(8)	17.034(2)
<i>c</i> /Å	18.173(9)	32.237(3)
$\alpha$ /°	80.66(1)	90
$\beta$ /°	68.33(1)	96.493(2)
$\gamma$ /°	85.25(1)	90
Volume/Å <sup>3</sup>	4202(4)	4698.8(8)
<i>Z</i>	1	4
$\rho_{\text{calc}}$ /cm <sup>3</sup>	1.359	1.517
$\mu$ /mm <sup>-1</sup>	1.093	1.468
<i>F</i> (000)	1765.0	2188.0
Crystal size/mm <sup>3</sup>	0.246 × 0.168 × 0.146	0.359 × 0.07 × 0.06
Radiation	MoK $\alpha$ ( $\lambda$ = 0.71073)	MoK $\alpha$ ( $\lambda$ = 0.71073)
2 $\theta$ range for data collection/°	5.64 to 52.76	6.12 to 50.054
Index ranges	-17 ≤ <i>h</i> ≤ 17, -22 ≤ <i>k</i> ≤ 22, 0 ≤ <i>l</i> ≤ 22	-10 ≤ <i>h</i> ≤ 10, -20 ≤ <i>k</i> ≤ 20, -38 ≤ <i>l</i> ≤ 38
Reflections collected	52608	78661
Independent reflections	17116 [ <i>R</i> <sub>int</sub> = 0.0692, <i>R</i> <sub>sigma</sub> = 0.0894]	8296 [ <i>R</i> <sub>int</sub> = 0.1467, <i>R</i> <sub>sigma</sub> = 0.0715]
Data/restraints/parameters	17116/33/985	5601/852/623
Goodness-of-fit on <i>F</i> <sub>2</sub>	1.020	0.987
Final <i>R</i> indexes [ <i>I</i> ≥ 2 $\sigma$ ( <i>I</i> )]	<i>R</i> <sub>1</sub> = 0.0661, <i>wR</i> <sub>2</sub> = 0.1345	<i>R</i> <sub>1</sub> = 0.0662, <i>wR</i> <sub>2</sub> = 0.1637

Final R indexes [all data]	R <sub>1</sub> = 0.1132, wR <sub>2</sub> = 0.1543	R <sub>1</sub> = 0.1053, wR <sub>2</sub> = 0.1916
Largest diff. peak/hole / e Å <sup>-3</sup>	0.63/-0.48	1.50/-1.08

**Table S2.** Selected interatomic distances (Å) and angles (°) for [1].

Cu1...Cu2	3.451(2)	Cu1O1Cu2	118.34(15)
Cu2...Cu3	3.417(1)	Cu3O1Cu1	108.47(14)
Cu3...Cu1	3.243(1)	Cu3O1Cu2	117.23(15)
Cu1...Cu4	5.228(3)	Cl1Cu1Cl4	110.08(5)
Cu1-Cl1	2.307(2)	O1Cu1Cl1	162.63(10)
Cu1-Cl4	2.744(2)	N4Cu1N5	175.51(15)
Cu1-O1	2.007(3)	N5Cu1Cl4	94.90(11)
Cu1-N4	1.948(4)	O1Cu2Cl2	167.44(10)
Cu1-N5	1.950(4)	N6Cu2N1	160.43(14)
Cu2-Cl2	2.258(1)	O1Cu3Cl3	169.34(10)
Cu2-O1	2.012(3)	N3Cu3N2	163.27(15)
Cu2-N1	1.951(3)	N7Cu4N7 <sub>1</sub>	180.0
Cu2-N6	1.949(3)	N9Cu4N9 <sub>1</sub>	91.62(14)
Cu3-Cl3	2.251(2)		
Cu3-O1	1.990(3)		
Cu3-N2	1.957(3)		
Cu3-N3	1.953(4)		
Cu4-N7	2.017(4)		
Cu4-N9	2.019(3)		
Cu4-Cl4	2.792(2)		

*i*-*x*, 2-*y*, 1-*z*

**Table S3.** Selected interatomic distances (Å) and angles (°) for [2].

Cu1...Cu2	3.386(1)	Cu1O1Cu2	116.79(18)
Cu2...Cu3	3.470(1)	Cu1O1Cu3	115.8(2)
Cu3...Cu1	3.389(1)	Cu2O1Cu3	119.10(18)
Cu1-O1	1.976(4)	O1Cu1N13	174.73(19)
Cu1-N1	1.941(5)	N1Cu1N13	90.9(2)
Cu1-N12	1.935(5)	N12Cu1N1	171.0(2)
Cu1-N13	1.982(5)	N12Cu1N13	92.5(2)
Cu2-O1	2.000(4)	O1Cu2N13 <sub>1</sub>	110.69(18)

Cu2-N2	1.943(5)	N2Cu2N3	92.6(2)
Cu2-N3	2.002(6)	N2Cu2N6	174.9(2)
Cu2-N6	1.963(5)	N2Cu2N13 <sub>1</sub>	89.01(19)
Cu2-N13 <sub>1</sub>	2.322(5)	N3Cu2N13 <sub>1</sub>	100.2(2)
Cu3-O1	2.024(4)	N6Cu2N3	92.2(2)
Cu3-N3 <sub>2</sub>	2.422(5)	N6Cu2N13 <sub>1</sub>	91.74(19)
Cu3-N7	1.974(5)	N7Cu3N3 <sub>2</sub>	91.59(19)
Cu3-N8	1.974(6)	N8Cu3N3 <sub>2</sub>	100.8(2)
Cu3-N11	1.948(5)	N8Cu3N7	92.1(2)
		N11Cu3N3 <sub>2</sub>	90.59(19)
		N11Cu3N7	173.6(2)
		N11Cu3N8	93.4(2)

$i1-x, 2-y, 1-z, z2-x, 2-y, 1-z$

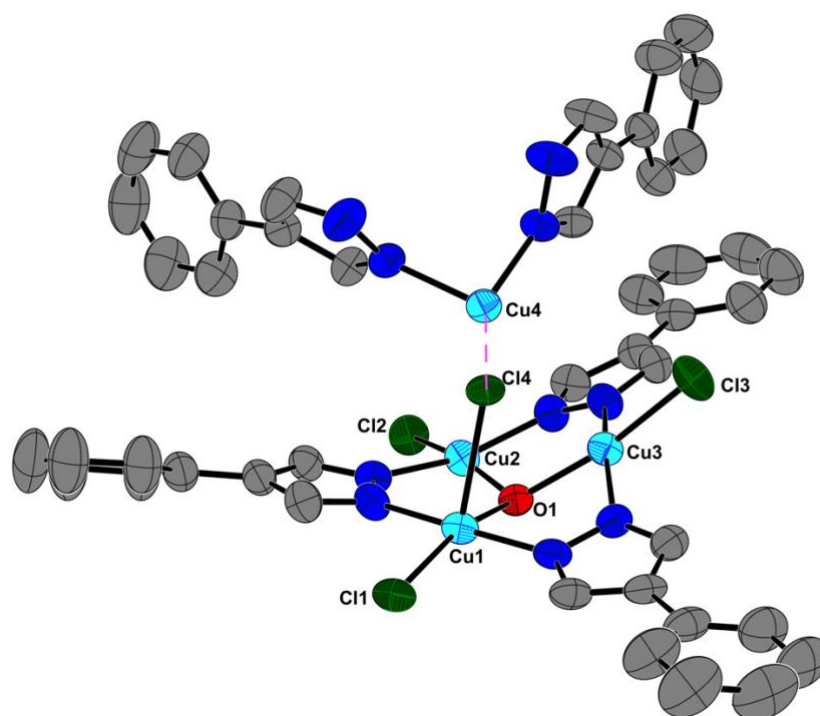


**Figure S1.** Asymmetric unit of [1] showing partial atom labeling scheme; thermal ellipsoids are drawn at 50% probability level. H-atoms, PPN counterion and interstitial solvents are not shown.

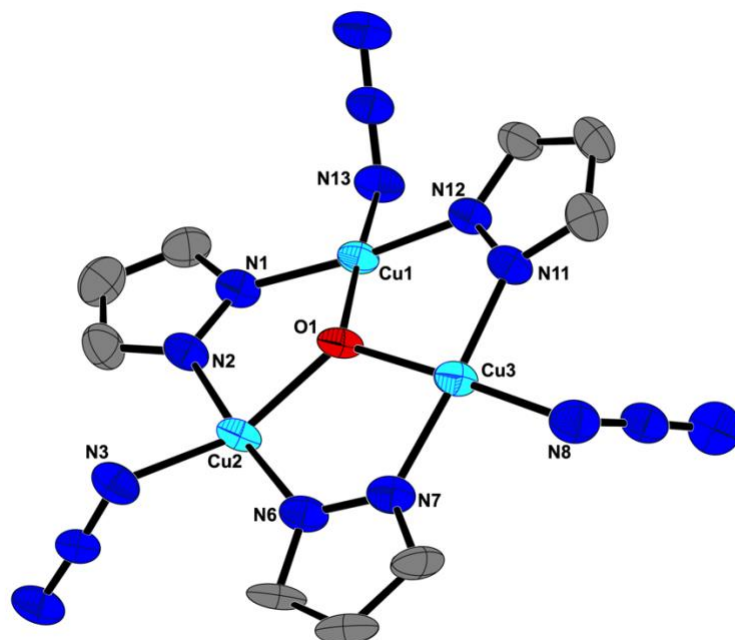


**Figure S2.** Molecular structure of [2] showing partial atom labeling scheme; thermal ellipsoids are drawn at 50% probability level. Azide disorder, H-atoms and PPN counterions are not shown for clarity.

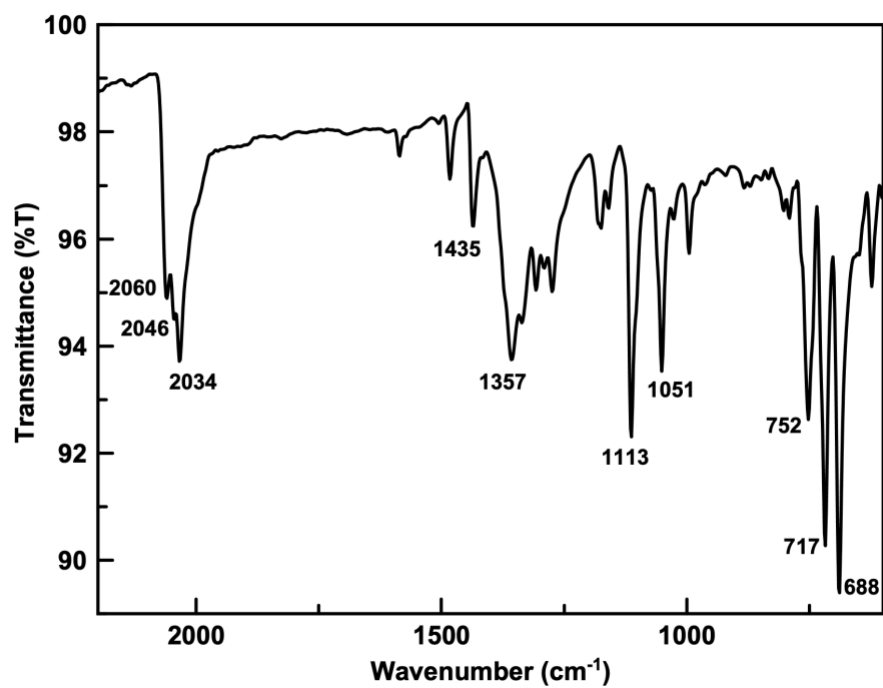


**Figure S3.** Infrared spectrum of [2] recorded in ATR mode.

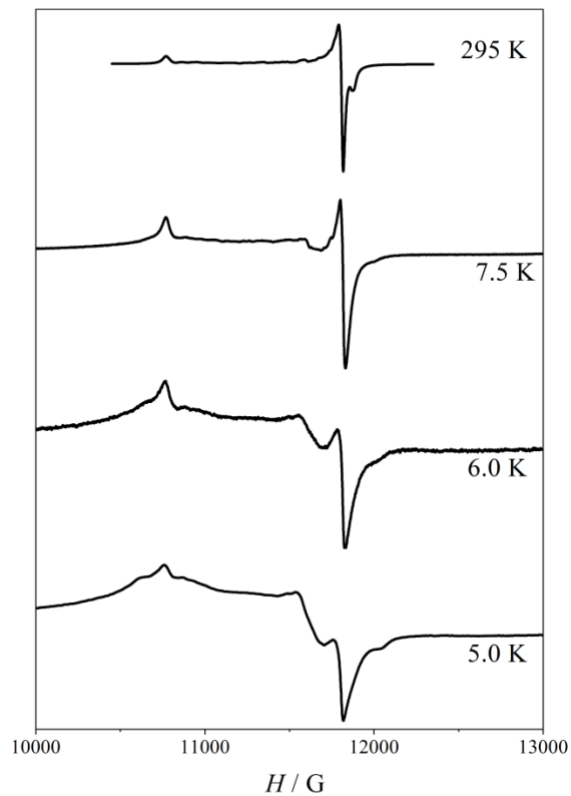


**Figure S4.** Solid-state X-band EPR spectra of [1] between 5 and 295 K.

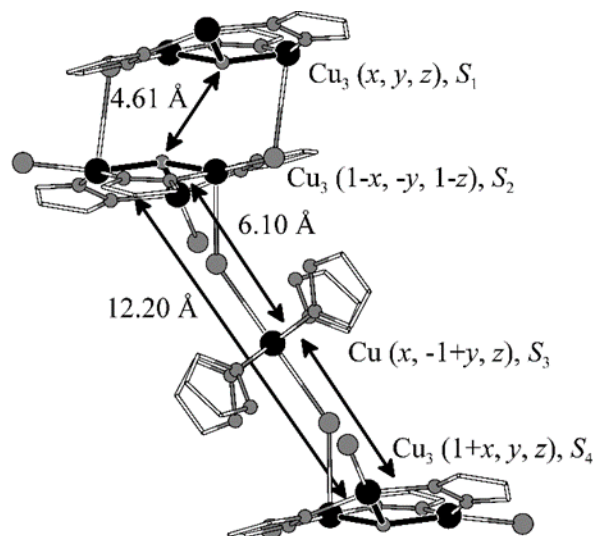


**Figure S5.** Dipolar exchange scheme indicating the symmetry codes of the spins  $S_i$  ( $i = 1-4$ ) and the main intermolecular distances of [1].